JOURNAL OF CATALYSIS 43, 168–180 (1976)

The Role of Heterogeneity in the Kinetics of a Surface Reaction

II. Kinetics of Decomposition of Isopropyl Methylphosphonofluoridate Adsorbed on γ-Alumina[1]

J. J. G. M. VAN BOKHOVEN, A. E. T. KUIPER,[2] AND J. MEDEMA

Chemical Laboratory TNO, POB 45, Rijswijk (ZH), The Netherlands

Received November 15, 1974; revised December 15, 1975

Rate data on the decomposition of isopropyl methylphosphonofluoridate (sarin) adsorbed on γ-alumina as well as on magnesia and carbon black impregnated with chromium trioxide, are obtained from microcalorimetric measurements. Normal *n*th order rate equations fail in properly describing the experimental results. Resemblance of the kinetics to Zeldovich kinetics leads to a rate model that is primarily characterized by a variation in activation free energy for the decomposition reaction. The model is consistent with the experimental rate data.

INTRODUCTION

Qualitative aspects of the adsorption and decomposition of isopropyl methylphosphonofluoridate (IMPF or sarin) on γ-Al_2O_3 have been studied by ir spectroscopy and are described in Part I (*1*). Adsorption of sarin appeared to take place irreversibly through bonding of the phosphoryl oxygen to a Lewis acid site. Decomposition of the adsorbed sarin proceeds almost exclusively by exchange of the fluorine against a surface hydroxyl group. The products of the reaction, viz. hydroxysarin and hydrogen fluoride, are also strongly adsorbed species. As the reaction proceeds entirely in the adsorbed phase, kinetic measurements are difficult. In a method applied by Kuiper (*2*) the amount of unreacted sarin is extracted and measured as a function of time; the method yields valuable information but its inherent experimental error is too large to allow a reliable establishment of the kinetic behavior of the reaction. Data from these extraction experiments are used to estimate the reaction enthalpy. It was thought feasible to develop a calorimetric technique to supply rate data of sufficient accuracy. The application of a calorimetric technique offers two advantages:

a. The reaction rate is measured *in situ.*
b. The method is usable irrespective of the particular reaction system.

The basis of the applicability of a calorimeter for kinetic purposes is found in the relation:

$$\dot{Q} = -\frac{dc}{dt}(-\Delta H_r),$$

where $\dot{Q}$ is the measured heat development, $-(dc/dt)$ is the reaction rate and ΔH_r the reaction enthalpy. ΔH_r must be calibrated by comparison with results obtained with other techniques.

A distinct drawback of calorimetric techniques is the purely quantitative character of the measurement. For this reason the technique must be sustained by qualitative methods that verify the nature of the

---

[1] This work is part of the doctorate thesis by J. J. G. M. V. B., Eindhoven, 1974.

[2] Present address: Philips Research Laboratories, Eindhoven, The Netherlands.

process to be studied. Another disadvantage often met in calorimetric techniques applied for kinetic purposes, originates from the thermal inertia of the measuring cell. As response velocities are relatively small, line shapes of thermograms have a tendency to be distorted.

The calorimetric method that was developed for the system sarin–adsorbent has been described in detail elsewhere (*3*a, b). For $t > 100$ min, $\dot{Q}$ is directly measured with a conduction type of microcalorimeter. For lower times the thermograms need a correction for line shape broadening; this broadening is particularly serious due to the large adsorption heat effect. A calculation procedure based on Fourier analysis largely accomplishes this correction. For the system sarin–alumina the separation of the initial adsorption (chemisorption) effect on the one hand and the subsequent reaction on the other allows one to follow the reaction rate for times after $t = 20$ min. For the system sarin–magnesia pure reaction rates may be followed for $t > 60$ min. In the present paper the rate curves are presented without full description of the calorimetric background. Because the correction for line shape broadening could not be applied to all thermograms, the period with neat information on reaction rates is not equal for all experiments.

METHODS

Materials

The alumina, made available by Ketjen (AKZO Chemie Nederland, Amsterdam, The Netherlands) had a γ-type crystal structure. The specific surface area was 280 m^2/g. The material consisted of pellets which were grained to a powder; the sieve fraction between 0.25 and 0.50 mm was used.

Magnesia was prepared from inactive MgO according to a method described by Baird and Lunsford (*4*). The calcination temperature was limited to 400°C, providing a specific surface area of 180 m^2/g.

Carbon black was obtained from Cabot (Berre-l'Etang, France); it is known commercially as Regal 400. Impregnation with chromium oxide was performed by contacting the material with a chromium (VI) oxide solution in water. After filtration it was dried in vacuum at room temperature. The surface area of the carbon black amounted to 115 m^2/g and was hardly affected by the chromium oxide impregnation.

Both magnesia and carbon black samples were used as a finely divided powder.

The organophosphorus compounds were synthesized in our Laboratory according to procedures described in Ref. (*5*). The purity of the samples was 99% at least.

Apparatus

A schematic view of the apparatus is shown in Fig. 1. The calorimeter contains two identical measuring cells, each consisting of a reaction vessel (A) and a thermopile (B). The two thermopiles are built into an aluminum block (C) that operates as a heat sink; they are electrically connected oppositely in order to mitigate the influence of temperature fluctuations penetrating from the environment. The resulting thermo-emf, which is a proportional measure for the heat flow, is registered by the recorder (G). The external temperature fluctuations are attenuated by the insulation space (E) in between the inner and outer wall (F); this space is evacuated during an experiment. A long-term stability of 0.05 μV (corresponding to about 1 μW) is attainable by controlling the waterbath thermostat, which surrounds the calorimeter, within ±0.003°C.

The dosing system, made of glass, can be evacuated to a pressure of 10^{-5} Torr by means of a combined mercury diffusion–oil rotary pumping system (S), which is connected to the dosing system via a liquid nitrogen trap (T). The pressure in the vacuum system can be read from Pirani and Penning gauges (P, Q). Adsorbate

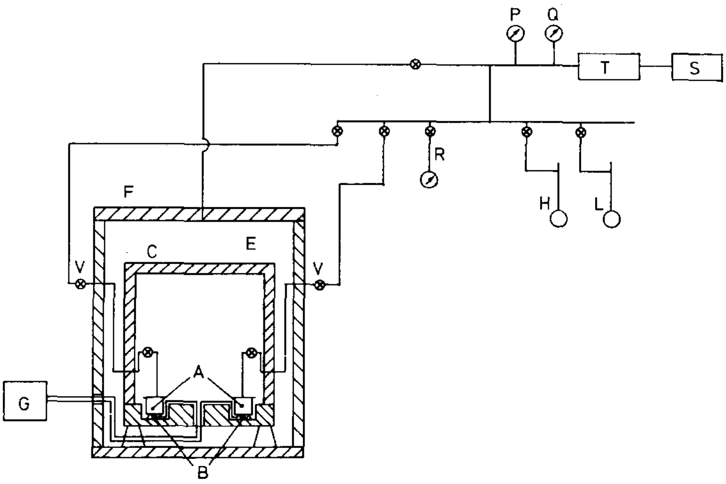

FIG. 1. The vapor dosing system and a schematic picture of the calorimeter. See text for explanation.

vapors are generated from the liquid phase in dosing vessels (H) or (L), which may be disconnected from the system. The pressure of the vapor is indicated by the Pirani gauge (R).

Procedure

In most cases the adsorbent samples (~1 g) were given a vacuum heat pretreatment; to this end the reaction vessels were connected to a separate vacuum system and were heated at temperatures up to 120°C. Then the reaction vessels were installed and the calorimeter was positioned in the thermostat for equilibration; this took between 10 and 18 hr, depending on the desired reaction temperature. Simultaneously the reaction vessels and insulation space were evacuated to pressures of 10^{-4} to 10^{-5} Torr. The valves (V) were closed to stop water vapor desorption from the adsorbents. After the heat flow signal had fallen to zero, a decomposition experiment was started.

By opening one of the valves (V) during 1–3 min sarin was dosed to one sample from the weighed and evacuated vessel (H) (saturated vapor pressure of sarin at room temperature is 2.4 Torr). The vessel (H) was cooled to −10°C in order to condense gaseous sarin from the dead space. From the new weight of vessel H the amount of adsorbed sarin was derived; these amounts were limited to between 35 and 250 mg.

The heat development resulting from adsorption and subsequent reaction was registered on punched tape in order to facilitate correction calculations.

After the heat flow had decreased sufficiently, the same procedure was followed for the other adsorbent sample.

RESULTS

Sarin adsorbed on alumina decomposes through two reactions, viz, hydrolysis or defluoridation and dealkylation. A change in enthalpy is coupled to each of these reactions as well as to the preceding adsorption. The actual heat of adsorption is considerable and appears in the thermogram as a very large signal. Although the rate of dealkylation is very small compared to defluoridation (*2*), the accompanying enthalpy change may not be ignored a priori. However, comparison of reaction heat developments by adsorbed sarin and some of its analogues with rates of dealkylation of the same systems, reveals that dealkylation does not contribute significantly to the measured heat flow signals (*3*a). So the reaction heat development may be interpreted as a measure of the defluoridation reaction only.

Rate equations of normal nth order reactions with or without poisoning or promoting effects of reaction products appeared not to apply to the experimental rate curves of defluoridation (*2*, *3*a). However, it was recognized that the type of kinetics often encountered in adsorption processes and known as Zeldovich kinetics, constitutes a basis for a satisfactory description of the experimental rate curves.

Zeldovich–Roginskii kinetics, which are often but less correctly designated as Elovich kinetics, generally apply to chemisorption processes (*6*, *7*). McLintock (*8*) mentions eight other processes (among which are graphitization of carbon and decomposition of surface formate on nickel) which obey the rate equation characteristic for Zeldovich kinetics:

$$\frac{dq}{dt} = ae^{-\alpha q}, \tag{1}$$

where q is the amount adsorbed (or decomposed) at time t, while a and α are constants which are adjusted for each experiment. In its integrated form Eq. (1) may be written as:

$$q = \frac{1}{\alpha} \ln (t + t_0) - \ln t_0, \tag{2}$$

where the constant $t_0 = 1/a\alpha$. The rate law is essentially an approximative mathematical description of a relationship between physical quantities without any claim on mechanistic background.

Whether rate data show adherence to Zeldovich kinetics is usually tested by means of Eq. (2). A plot of q vs $\ln t$ should yield a straight line for $t \gg t_0$, provided that the parameters a and α are correctly chosen. An alternative test is based on the equation derived from Eq. (2) by differentiation:

$$\frac{dq}{dt} = \frac{1}{\alpha (t + t_0)}. \tag{3}$$

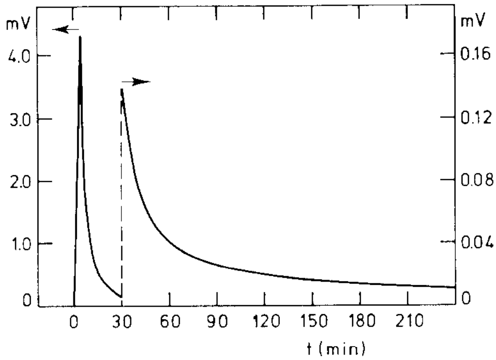

FIG. 2. Thermogram resulting from sarin adsorption on alumina; W_a = 25.2 mg; T_r = 0.6°C. The heat production is expressed in the measured thermo-emf. 1 mV corresponds to 16.6 mW.

For values of $t \gg t_0$ a proportional relation between rate and reciprocal time should be observed. In the present case it is more rational to examine the latter relation, because rate is a directly measured quantity. In graphical representations the product of rate and time will be shown hereafter; for $t \gg t_0$ this product should tend to a constant value.

For reasons of brevity and clarity only those experimental results are cited here that are relevant to the model that is postulated to underly the particular kinetics. A comprehensive description is given elsewhere (*3a*).

Figure 2 shows the heat development (not corrected for thermal inertia) resulting from a sarin adsorption on alumina. The heat produced by the adsorption itself takes about 100 min to flow to the heat sink. From this time on the registered heat originates from the defluoridation reaction only; moreover, it was shown that the distortion in the line shape is negligible for t > 100 min (*3*a).

Figure 3 shows part of the same thermogram in a $\dot{Q} \times t$ vs t plot. The horizontal part for large t values proves that the inverse proportionality between rate and time [expressed in Eq. (3) and valid for $t \gg t_0$] does apply. The relation is characterized by the value A', which is expressed in joules.

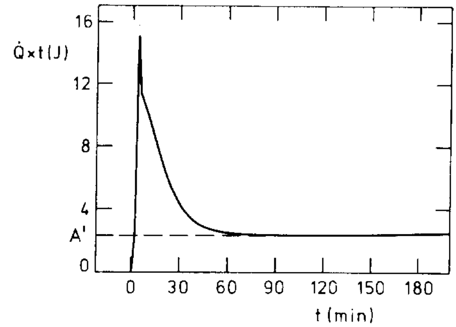

FIG. 3. The same experiment as in Fig. 2; product of rate ($\div \dot{Q}$) and time as a function of time. The horizontal part in the graph represents the inverse proportionality between rate and time.

The quantities A' of a number of sarin decompositions at 28°C on alumina pretreated at 28°C, are collected in Fig. 4 as a function of the amount adsorbed. The reaction rate is seen to be proportional to the amount adsorbed.

The proportional relation between $\dot{Q}$ and $1/t$ cannot extend to $t = 0$, because the reaction rate would become infinitely high. The Zeldovich equations preclude this infeasibility through the introduction of the quantity t_0. The horizontal line representing the product of rate and time in Fig. 3 must necessarily have a deviation downward at some point obscured by line shape distortion. Because important information was expected to be gained from the position of this point of deviation, further experiments were performed after two improvements had been introduced in the technique: the response velocity was raised and, in most cases, the distorted thermograms were corrected for thermal inertia.

The corrected results of decomposition experiments on alumina samples pretreated at 120°C are shown in Fig. 5 for five different reaction temperatures T_r. Except for $T_r = 40$°C the point of deviation from the inverse proportionality between r and t is evident: similar experiments have been performed on alumina previously exposed to a hydrogen fluoride atmosphere (Fig. 6), on magnesia samples pretreated at reaction temperatures of 10°C (Fig. 7a) and 30°C (Fig. 7b), and on carbon black impregnated with chromium (VI) oxide at a reaction temperature of 25°C (see Fig. 8).

The thermogram of the latter experiment has not been corrected for thermal inertia. All cited experiments reveal an inverse proportionality between rate and time in a definite period; except for the uncorrected thermogram measured for carbon black, the starting point of this period is visible.

Because of the kinetic features mentioned above, a model frequently used to explain Zeldovich kinetics was adopted as a starting point for clarifying the rate data.

DISCUSSION

Kinetic Model

Aharoni and Tompkins (7) mention a number of different physical models for adsorption processes all leading to adherence to Zeldovich kinetics. The basic features of the models are either a surface inhomogeneity (intrinsic or induced) or a variation in adsorption site number or both.

For the system sarin–adsorbent a variation in activation energy seems to be the more plausible point of departure to explain the experimental reaction rates. In order to leave open the a priori possibility that also the entropy of activation shows a variation, a distribution in the activation free energy of the reaction is postulated. The complete model that will be seen to be

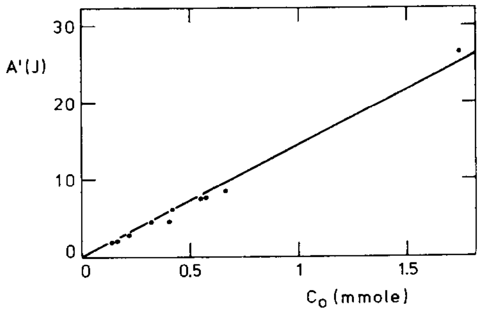

FIG. 4. The quantity A' (see Fig. 3) as a function of amount sarin adsorbed on alumina; $T_r = 28$°C.

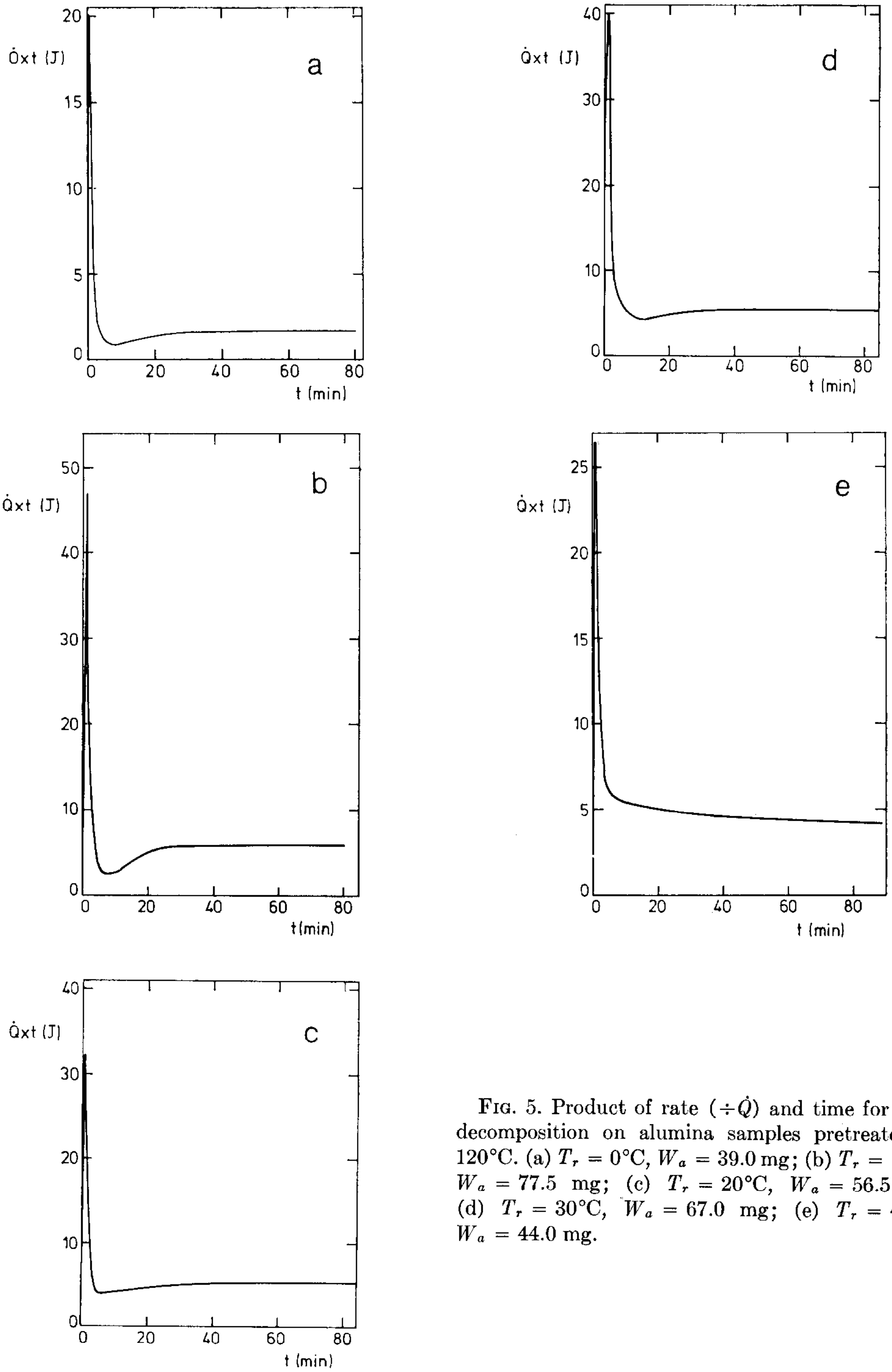

FIG. 5. Product of rate ($\div\dot{Q}$) and time for sarin decomposition on alumina samples pretreated at 120°C. (a) $T_r = 0°C$, $W_a = 39.0$ mg; (b) $T_r = 10°C$, $W_a = 77.5$ mg; (c) $T_r = 20°C$, $W_a = 56.5$ mg; (d) $T_r = 30°C$, $W_a = 67.0$ mg; (e) $T_r = 40°C$, $W_a = 44.0$ mg.

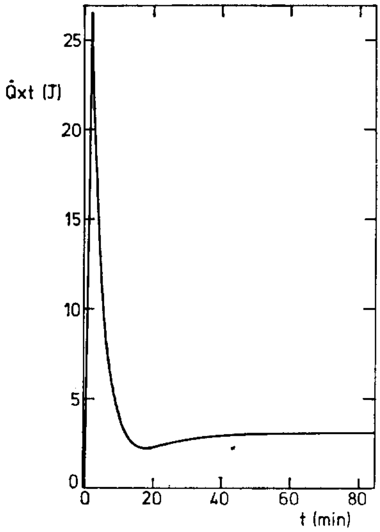

FIG. 6. Product of rate and time vs time for sarin decomposition on an alumina sample pretreated in a hydrogen fluoride atmosphere. $T_r = 20°C$; $W_a = 52$ mg.

consistent with the experimental results, is characterized by the following features:

1. The molecules decompose by a defluoridation reaction; the activation free energy involved in this reaction is not equal for all reacting molecules; on an average it increases in the course of the reaction.
2. Sarin molecules are immobile after adsorption.
3. For each fraction of molecules with the same activation free energy for decomposition the reaction is first order in sarin and zero in any other species.
4. The reaction enthalpy may be considered to be equal for all molecules.

Sub 1. Heterogeneity of the surface. Heterogeneity of surface sites on alumina is expressed in such features as differential heats of adsorption, variation in surface acidity and broad frequency intervals for surface OH-stretchings. With respect to sarin decomposition a scatter in strength of basic hydroxyls seems to be of particular interest, although a change in activation energy caused by the reaction products cannot be precluded a priori (induced heterogeneity).

In order to test the model a definite distribution function for the activation free energy has to be chosen, whether this distribution exists at the beginning of the reaction or develops gradually in the course of the reaction. For the sake of mathematical convenience a block-shaped distribution function will be assumed first: all activation free energies between the limits

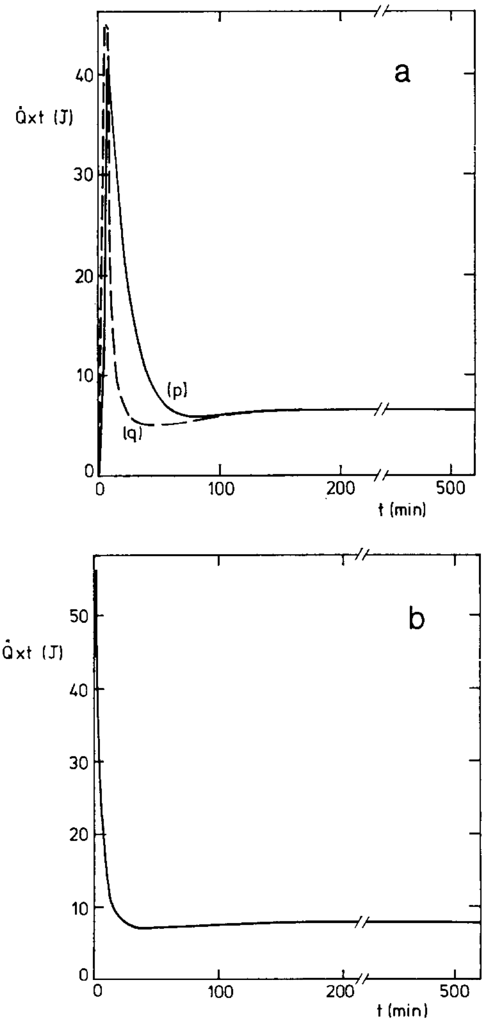

FIG. 7. (a) Product of rate and time vs time for sarin decomposition on magnesia pretreated at reaction temperature; $T_r = 10°C$, $W_a = 93.0$ mg; (*p*) not corrected for thermal inertia; (*q*) corrected for thermal inertia. (b) Product of rate and time vs time for sarin decomposition on magnesia pretreated at reaction temperature; $T_r = 30°C$, $W_a = 88.0$ mg.

G_1 and G_2 are supposed to occur with equal frequency. This choice is referred to as the "simple model" by Peers (*9*). The choice of this function is arbitrary; in Part III (*10*) it will be seen that this function shape may be derived directly from experimental results for a substantial part.

Sub 2. Conclusive evidence for the immobility of sarin adsorbed on oxidic adsorbents was obtained from a series of separate adsorption experiments with radioactively labeled sarin. These experiments are described in Ref. (*3a*).

Sub 3. Order of the reaction. First order kinetics in sarin for each fraction of molecules on a "patch" with one definite activation free energy, is a consequence of the mechanism argued in Part I (*1*).

It would be more precise to state that the reaction is first order in "reaction centers": a reaction center is thought to consist of an adsorbed sarin molecule plus neighboring hydroxyl groups. The center reacts when the activation free energy, specific to this center, is overcome. On account of the feature mentioned in sub 2, however, the numbers of reaction centers and sarin molecules are identical.

Sub 4. Because a distribution in reaction enthalpy cannot be regarded as less likely than a distribution in activation energy, an explicit statement on the nonvariation of the reaction enthalpy has to be made.

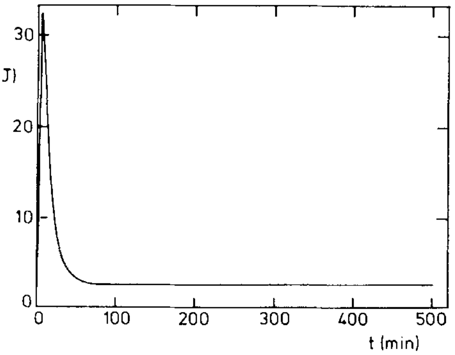

FIG. 8. Product of rate and time vs time for sarin decomposition on carbon black impregnated with chromium oxide (6.2 wt% chromium). Pretreatment and reaction temperature: 25°C, W_a = 72 mg.

TABLE I

Comparison of Extraction Experiments by Kuiper (*2*) and Calorimetric Experiments in Order to Find the Overall Reaction Enthalpy (ΔH_r)

Period (min)	Extraction expt; fraction decomposed (%)	Calorimetric expts; heat developed (J/mmole)	$-\Delta H_r$ (kcal/mole)
60–1370	14	43.8	75
60–2970	17	54.6	77
60–3095	20	55.2	66

If distributions both for activation enthalpy and for reaction enthalpy do exist, the mutual coupling between them determines whether the thermokinetic curves are distorted and, if so, how they are distorted. It is clear that there is no distortion in two cases: (i) if activation and reaction enthalpies are coupled randomly; (ii) if the reaction enthalpy is constant.

For a series of analogous reactants in one type of reaction something is known on the relation between reaction enthalpy and activation energy. Glasstone *et al.* (*11*) concluded on the basis of "potential energy profiles" that there is an antibatic relation between the activation energy and the reaction enthalpy. This relation has been observed for reactions of halogen hydrocarbons with sodium vapor. It is valid also for substitution reactions in organophosphorus compounds (*12*); for a series of halogenide substituents the reaction enthalpy decreases with increasing activation energy, provided that solvation effects are corrected for. So, for a series of analogous reactants the activation and reaction enthalpies seem to be related.

In the present system identical instead of analogous molecules and groups are involved. In this respect a comparison with adsorption processes is more appropriate. However, no generally valid relation between activation and reaction enthalpies for adsorption has been established, although several different relations have been argued (*9*). Experimental evidence seems to be entirely lacking.

For this reason no particular relation between the distributions may be assumed; the statement that the reaction enthalpy is constant is probably not too unacceptable in view of the approximate calibration results shown in Table 1.

In view of the relative error of 10% in the calculated reaction enthalpies, it may be concluded that a considerable variation in reaction enthalpy is unlikely.

Derivation of the Rate Equation

The model given above permits a straightforward derivation of the kinetic equation; it parallels the procedure followed by Peers (*9*) for chemisorptions.

Let an amount of sarin (c^0) be adsorbed at time $t = 0$, resulting in a system of reaction centers that possesses a block-shaped distribution function in activation free energies [$\rho(G)$] between the extreme values G_1 and G_2. The values are related to reaction rate constants k_1 and k_2, respectively, through:

$$k_1 = (k_b T/h)\exp(-G_1/RT)$$

and

$$k_2 = (k_b T/h)\exp(-G_2/RT).$$

The distribution function is normalized by the condition

$$\int_0^\infty \rho(G)dG = 1.$$

Therefore $\rho(G) = 1/(G_2 - G_1)$ for $G_1 < G < G_2$ and $\rho(G) = 0$ outside this interval.

The initial amount of sarin in a narrow interval ΔG around G is given by

$$\Delta c_G{}^0 = \frac{c^0 \Delta G}{G_2 - G_1}. \qquad (4)$$

These molecules, having to surmount an activation free energy G, decompose according to the kinetic equation

$$-\frac{d(\Delta c_G)}{dt} = k_G \Delta c_G$$

or

$$\Delta c_G = \Delta c_G{}^0 e^{-k_G t}. \qquad (5)$$

The total velocity of sarin decomposition is found by summation between G_1 and G_2:

$$r = \sum_G -\frac{d(\Delta c_G)}{dt} = \sum_G k_G c_G{}^0 e^{-k_G t}. \qquad (6)$$

Insertion of Eqs. (4) and (5) into (6) leads to:

$$r = \frac{c^0}{G_2 - G_1} \sum_G k_G e^{-k_G t} \Delta G.$$

Because the activation free energy is assumed to vary continuously between G_1 and G_2 the summation may be transformed into an integration:

$$r = \frac{c^0}{G_2 - G_1} \int_{G_1}^{G_2} k_G e^{-k_G t} dG.$$

After replacement of the integration variable G by k using the relation $dG = (-RT/k)dk$ it follows that:

$$r = \frac{-RTc^0}{G_2 - G_1} \int_{k_2}^{k_1} e^{-kt} dk \qquad (7)$$

$$= \frac{RTc^0}{G_2 - G_1} \frac{1}{t}(e^{-k_2 t} - e^{-k_1 t}). \qquad (8)$$

The feasibility of Eq. (8) is checked as follows: (i) Expansion of the exponentials

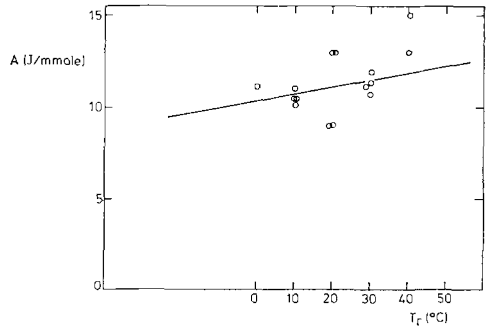

FIG. 9. Variation of the quantity A with reaction temperature for alumina samples pretreated at temperatures between 75 and 120°C.

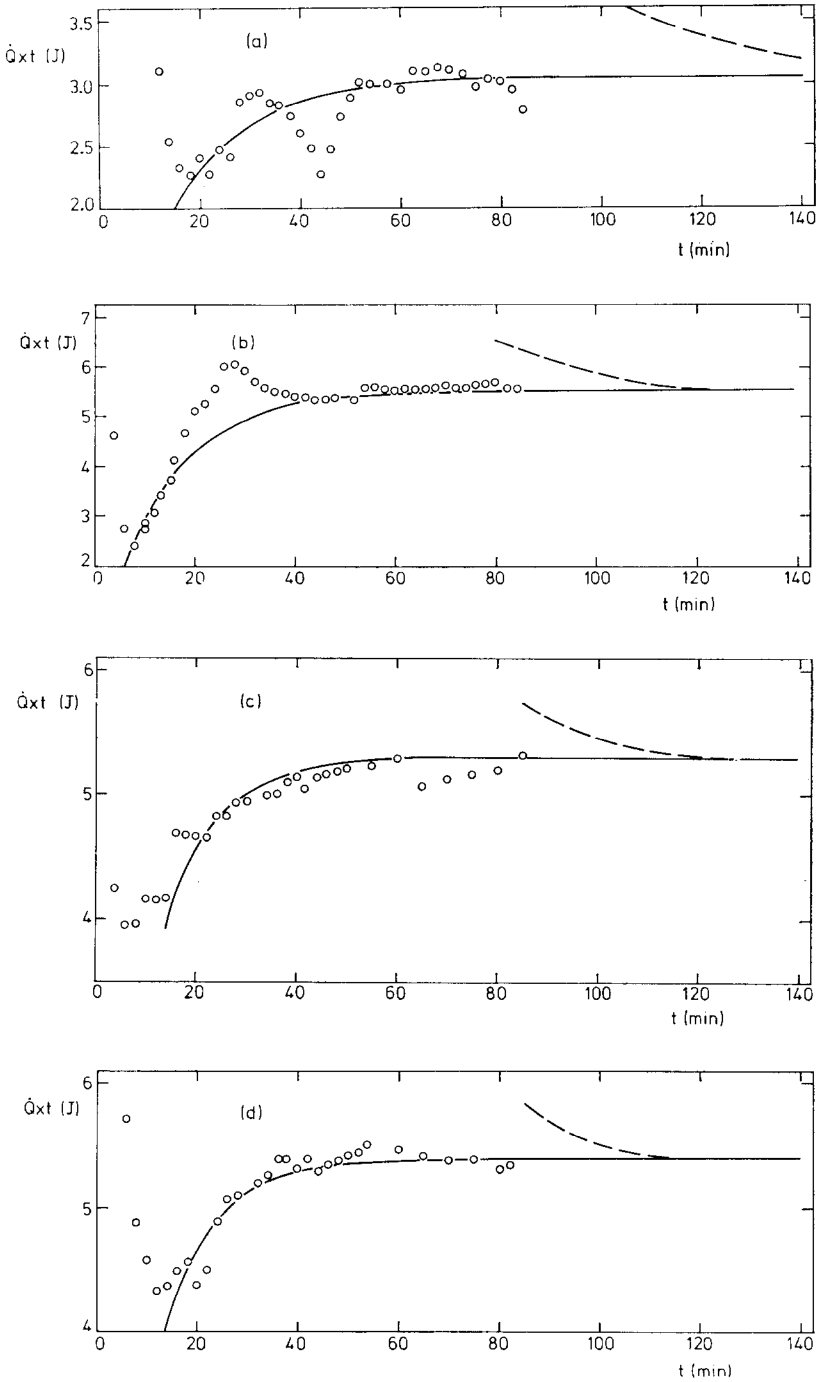

FIG. 10. Fitting functions of the form $A\{1 - \exp(-k_1t)\}$ for sarin decompositions on alumina samples pretreated at 120°C. (○) Experimental data corrected for thermal inertia; (– – –) experimental data not corrected for thermal inertia; (——) fitting curve. Conditions: (a) $T_r = 0°C$, $W_a = 39.0$ mg; (b) $T_r = 10°C$, $W_a = 77.5$ mg; (c) $T_r = 20°C$, $W_a = 56.5$ mg; (d) $T_r = 30°C$, $W_a = 67.0$ mg.

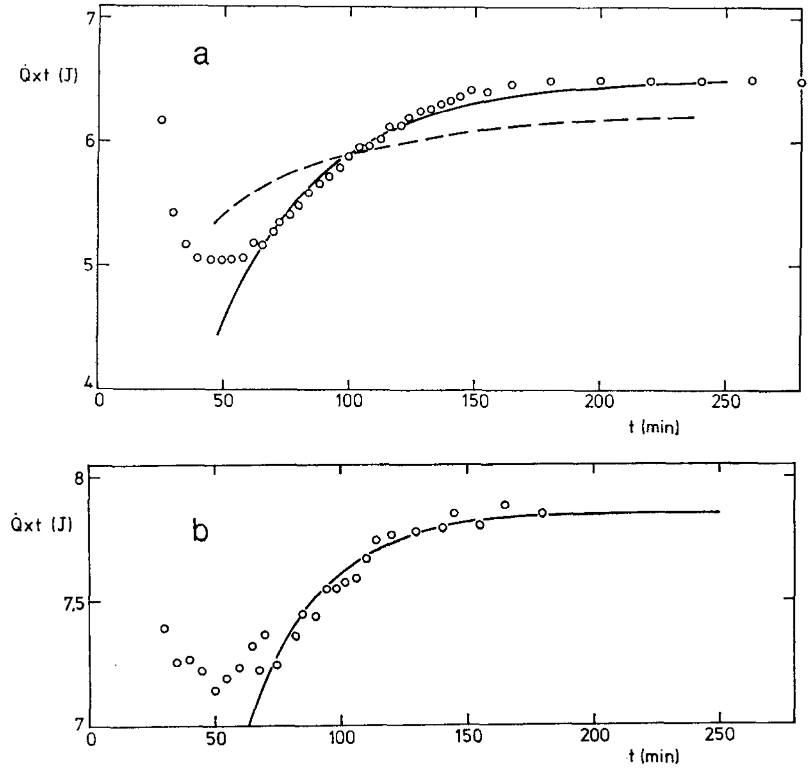

FIG. 11. Fitting functions of the form $A\{1 - \exp(-k_1t)\}$ for sarin decompositions in magnesia samples pretreated at reaction temperature. (○) Experimental data; (——) fitting curve; (– – –) best fitting curve, if the reaction is assumed to be second order (maintaining the distribution in G). (a) $T_r = 10°\text{C}$, $W_a = 93.0$ mg; (b) $T_r = 30°\text{C}$, $W_a = 88.0$ mg.

into series easily shows that

$$\lim_{t\to 0} r = RTc^0/(G_2 - G_1);$$

this is exactly the result of integration of Eq. (7) for the particular case $t = 0$. (ii) Integration of r between $t = 0$ and ∞ may be verified to yield c^0, as is to be expected.

Two factors will be discerned to examine whether Eq. (8) describes the experimental results:

a. The time independent factor $A = RTc^0(-\Delta H_r)/(G_2 - G_1)$, which has to be identified with the earlier defined quantity A' for $c^0 = 1$ mmole; A is expressed in J/mmole.

b. The factor $\{\exp(-k_2t) - \exp(-k_1t)\}/t$ which accounts for the time dependence of the reaction rate.

Sub a. The factor A is shown as a function of temperature in Fig. 9. All experiments on Al_2O_3 samples pretreated at temperatures between 75 and 120°C, have been included in this graph, as no significant influence from pretreatment temperature was observed. The best fitting straight line through the origin according to the least squares method is presented in Fig. 9. The slope of this line is characterized by a standard deviation of 2.5%, indicating that the experimental temperature dependence of the factor A satisfactorily corresponds to that predicted by the model.

In the comparison of the quantities A it is implicitly assumed that the distribution of the sarin molecules over the surface sites during adsorption is temperature independent; on the basis of this assumption $G_1 - G_2$ may be taken as a constant. The hypothesis is supported by the ir spectroscopic evidence (*1*) that the surface coverage and structure of sarin are independent of the pretreatment temperature of the alumina sample.

Sub b. The time dependence of the factor $\{\exp(-k_2t) - \exp(-k_1t)\}/t$ is strongly influenced by the magnitudes of the parameters k_1 and k_2. Provided k_2 is sufficiently small and k_1 sufficiently large, the sum of the exponentials may be replaced by unity in a definite time interval. As the reaction rate is inversely proportional to time for $50 < t < 3000$ min, these conditions may be considered to be fulfilled. $\text{Exp}(-k_2t)$ being negligibly small, the factor may be replaced by $\{1 - \exp(-k_1t)\}/t$. Functions of this form have been fitted to the experimental curves by adapting the value of k_1. The results for sarin decompositions at 0, 10, 20, and 30°C are shown in Fig. 10. In this figure the inverse proportionality between rate $(\div \dot{Q})$ and time appears from the horizontal line in the interval $50 < t < 140$ min.

The results for magnesia at reaction temperatures 10 and 30°C are shown in Fig. 11. The resulting k_1 values for alumina and magnesia are plotted vs $1/T$ in Fig. 12. From the slope and intersection with the ln k axis of the best fitting straight line, the frequency factor k_0 and the activation enthalpy ΔH_{act} of the fastest reacting "reaction centers" may be derived. The values are as follows:

	k_0 (sec^{-1})	ΔH_{act} (kcal/mole)
Al_2O_3	2	4.3
MgO	0.5	4.2

Both for the time dependence and the temperature influence it may be concluded that Eq. (8) satisfactorily predicts the experimental rate, thus confirming the postulated model.

The physical interpretation of the extremely small frequency factor requires particular attention. Together with considerations concerning the shape and the origin of the distribution in G this will be discussed in Part III (*10*).

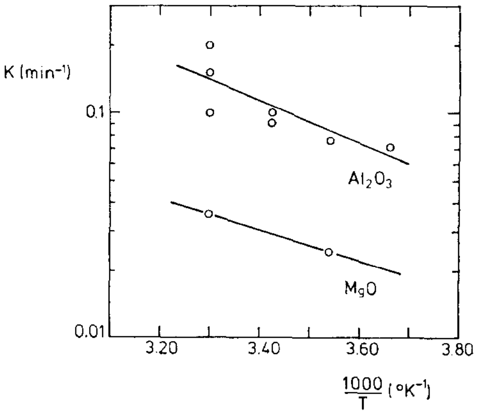

FIG. 12. Logarithmic plots of k_1 vs reciprocal temperature for alumina pretreated at 120°C and magnesia pretreated at reaction temperature.

CONCLUSION

Normal *n*th order rate equations fall short in reflecting the decomposition rate of sarin adsorbed on alumina, magnesia or carbon black impregnated with chromium (VI) oxide. A kinetic model that is primarily characterized by a variation in activation free energy, is able to describe the rate data adequately. The tentative assumption that the distribution function of the activation free energies is block-shaped is confirmed by experimental results. The kinetics bear a resemblance to the well-known Zeldovich–Roginskii kinetics of adsorption and chemisorption processes.

ACKNOWLEDGMENTS

The authors greatly appreciated the always stimulating discussions with Professor G. C. A. Schuit. The assistance offered by Mr. H. Bakker, Mrs. C. Plasse-Nederpel, and Mr. H. Orriens in experimental and computational work was essential to the investigations.

REFERENCES

1. Kuiper, A. E. T., Van Bokhoven, J. J. G. M., and Medema, J., *J. Catal.* **43,** 154 (1976).
2. Kuiper, A. E. T., thesis, Eindhoven, 1974.
3. (a) Van Bokhoven, J. J. G. M., thesis, Eindhoven, 1974; (b) *J. Phys. E, Sci. Instrum.* **9,** 123 (1976).
4. Baird, M. J., and Lunsford, J. H., *J. Catal.* **26,** 440 (1972).

5. Houben, J., and Weijl, T., "Methoden der Organischen Chemie," Part 1. Thieme Verlag, Stuttgart, 1963.
6. Low, M. J. D., *Chem. Rev.* **60**, 267 (1960).
7. Aharoni, C., and Tompkins, F. C., *in* "Advances in Catalysis" (D. D. Eley, H. Pines and P. B. Weisz, Eds.), Vol. 21, p. 1. Academic Press, New York, 1970.
8. McLintock, I. S., *J. Catal.* **16**, 126 (1970).
9. Peers, A. M., *J. Catal.* **4**, 499 (1965).
10. Van Bokhoven, J. J. G. M., Kuiper, A. E. T., and Medema, J., *J. Catal.* **43**, 181 (1976).
11. Glasstone, S., Laidler, K. J., and Eyring, H., "The Theory of Rate Processes." McGraw-Hill, New York, 1941.
12. Hudson, R. F., "Structure and Mechanism in Organophosphorus Chemistry," p. 92. Academic Press, London, 1965.